

AperTO - Archivio Istituzionale Open Access dell'Università di Torino

Comparative study of naphthalene adsorption on activated carbon prepared by microwave-assisted synthesis from different typical coals in Xinjiang

This is the author's manuscript

Original Citation:

Availability:

This version is available <http://hdl.handle.net/2318/1634644> since 2017-07-13T16:37:52Z

Published version:

DOI:10.1016/j.jtice.2015.09.001

Terms of use:

Open Access

Anyone can freely access the full text of works made available as "Open Access". Works made available under a Creative Commons license can be used according to the terms and conditions of said license. Use of all other works requires consent of the right holder (author or publisher) if not exempted from copyright protection by the applicable law.

(Article begins on next page)

23 **Abstract:**

24 Coal-based activated carbons (CACs) prepared from anthracite (A) coal, bituminous (B)
25 coal, and long flame (L) coal (i.e., ACAC, BCAC, and LCAC) from Xinjiang, China, using
26 KOH as activating reagent, were investigated under various microwave radiation power
27 levels. The results show that the adsorption capacity of the obtained activated carbons
28 (prepared under the optimum power level) towards naphthalene follows the order: ACAC >
29 BCAC > LCAC. In addition, the textural properties of the CACs were investigated by
30 means of SEM and low-temperature N₂ adsorption. The surface chemistry features of the
31 CACs were investigated by XPS, FTIR spectroscopy and Boehm's titration method. ACAC
32 has a higher surface area, pore volume, and zero point charge (pH_{PZC}) than the BCAC and
33 LCAC, while acidic oxygen functional group of the ACAC is lower than that of BCAC and
34 LCAC. In addition, the adsorption of naphthalene from the aqueous solution on the CACs
35 could be favorably described by the Freundlich isotherm. The adsorption kinetics fits very
36 well to the pseudo-second-order model. Among the three coals, A-coal was the best
37 material having low ash content and less than 10% volatile content, which is beneficial for
38 the preparation of CAC using microwave -assisted synthesis for naphthalene adsorption.

39 **Keywords:** Microwave radiation; Activated carbons; Adsorption; Naphthalene

40

41

42

43

44

45 **1. Introduction**

46 Activated carbon (AC), which is a crude form of graphite carbonaceous adsorbents is
47 known for its high porous surface area, controllable pore structure, and low acid or base
48 reactivity, making it widely used as a gas-phase and liquid-phase adsorbent [1]. One of the
49 main challenges in the commercial manufacture of AC is to identify new precursors that are
50 cheap, accessible and available in abundant quantities. Such precursors would have a
51 potential for significant economic benefits. Many raw lignocellulosic materials such as rice
52 husk [2], Jatropha hull [3], pistachio nut shells [4], cassava peel [5], bamboo [6], bean pods
53 [7] and wood [1] have been used for the preparation of AC and have had different degrees
54 of success over the years. However, some of these raw materials are difficult to collect and
55 have an unstable source. Recently, coals (being the first known precursor for AC) have
56 become again popular as raw materials for the production of AC because of their not very
57 high price and wide prevalence [8].

58 Among all provinces in China, Xinjiang province has the largest coal-producing area, the
59 coals from which have different properties. The production of coal enormously increased,
60 exceeding 1.6 million tons in 2013. Thus, the selection of coal as a stable alternative
61 material for the preparation of AC in Xinjiang is significant.

62 The preparation of AC generally involves physical or chemical activation methods under
63 high temperature by heating [5, 6]. Conventional electric furnace heating is the common
64 method for AC production, and this method usually takes several hours and does not ensure
65 a uniform temperature for various sizes and shapes of samples. In recent years, microwave
66 radiation has emerged as a promising alternative method to heat materials. Microwave

67 heating has been increasingly utilized in various technological and scientific fields for a
68 variety of applications, because of its advantages; microwave heating affords faster and
69 uniform heating rate and readily transforms to heat inside the particles by dipole rotation
70 and ionic conduction as compared with conventional heating method [9, 10]. Nevertheless,
71 according to the literature, information is lacking on preparation of AC from different kinds
72 of coal under microwave radiation.

73 Polycyclic aromatic hydrocarbons (PAHs) always occur in oil, coal and tar deposits. In
74 addition, the compounds are formed from the incomplete combustion of carbon-containing
75 fuels, which are the most widespread organic pollutants. PAHs in the environment are
76 found primarily in soil, sediment and oily substances. These compounds can enter water
77 bodies through atmospheric deposition, urban runoff and sewage discharges. As a class of
78 environmental pollutants, PAHs are a problem because some have been identified as
79 carcinogenic, mutagenic and teratogenic [11]. Currently, various methods have been used to
80 remove PAHs in water; these methods include adsorption, biodegradation and sonication
81 [12, 13]. Moreover, adsorption has proved to be one of the most attractive techniques for
82 removing PAHs using AC from aqueous solutions. Cabal et al. [7] studied the adsorption of
83 naphthalene onto bean pod-derived carbons and found that carbon composition that
84 includes mineral matter might play an important role in naphthalene retention. Yuan et al.
85 [14] prepared a series of porous carbons and used them for PAHs adsorption, and results of
86 experiments showed that the equilibrium data fit the non-linear Freundlich equation well
87 and the adsorption of PAHs appeared to be a two-stage process controlled by diffusive
88 transport processes. Iovino P et al. [15] studied single and competitive adsorption of toluene

89 and naphthalene onto activated carbon was fitted the Freundlich equation well. Thus, the
90 preparation of coal-based activated carbons (CACs) from suitable types of coal in Xinjiang
91 by microwave induction and their application in naphthalene adsorption from aqueous
92 solution are important.

93 The main objectives of this study were to prepare AC from coals by microwave
94 radiation and to evaluate the feasibility of using the produced AC to remove PAHs from
95 aqueous solutions. Three kinds of typical Xinjiang coals (anthracite (A)-coal, bituminous
96 (B)-coal and long flame (L)-coal) with KOH as activator were used to prepare AC. The
97 influence of microwave power on the adsorption capacities of the CACs for naphthalene
98 was investigated, enabling the process conditions for preparing CACs with
99 high adsorption properties to be determined. In addition, the relationship between some
100 properties including the BET surface area, pore volume, pH_{PZC} and surface groups, as well
101 as the structures of CACs were investigated. Naphthalene, which is one of the most
102 abundant PAHs in wastewater, was chosen as the target pollutant.

103 **2. Experimental**

104 **2.1. Raw materials**

105 These raw coals (A-coal, B-coal and L-coal) were purchased from TBEA, Xinjiang
106 Uygur Autonomous Region, China. The coals were crushed and sieved to 100 meshes. The
107 resultant coals were washed four times with distilled water to remove dust and dried in an
108 air oven at 110 °C for 4 h. After cooling, the powdered coals were stored in a glass jar at
109 room temperature. All reagents used were of analytical grade. The proximate analysis of
110 coal was determined by standard test method (GB/T 212-2008). The selected

111 physico-chemical properties of A-coal, B-coal and L-coal are shown in Table 1.

112 **Table 1 should be positioned here.**

113 **2.2. Preparation of CACs**

114 CACs were prepared within a microwave oven (MM823LA6-NS, Midea) at a frequency
115 of 2.45 GHz. The 10 g mixture of various ratios of dried coal powder with the activator
116 (KOH) was placed in a quartzose tube of a microwave reactor for activation under vacuum
117 atmosphere at a given power level (300, 500, 700 and 900 W). The resulting products were
118 washed with 10% hydrochloric acid and distilled water until the filtrate reached a neutral
119 state. The preparation parameters of preparation for CACs from different kinds of
120 coals were decided based on the optimum conditions reported in previous literatures [16,
121 17].

122 **2.3. Characterization methods**

123 Elemental analysis of carbon, hydrogen and nitrogen was carried out using a VarioEL III
124 analyzer. Sulfur content was determined by Eshka method (GB/T 214-2007). The ash
125 content was determined according to proximate analysis of coal (GB/T 212-2008) and the
126 standard test method for granular activated carbon. The oxygen content was determined by
127 difference.

128 The XPS analysis was conducted using a PHI5700 ESCA system equipped with a Mg K_{α}
129 X-ray source (1253.6 eV) under a vacuum pressure $< 10^{-6}$ Pa. Pass energy was set as 187.85
130 and 29.35 eV for the survey and high-resolution spectra, respectively. The XPS spectra of
131 the CACs were calibrated by taking the graphitic peak as 284.6 eV.

132 The surface morphology of the CACs was examined using scanning electron microscopy

133 (SEM) (JSM-6490LV, Japan) at accelerating voltages of 15 KV. Before observation, the
134 CACs were coated with gold in E-1010 Ion sputter.

135 The textural properties of the CACs were characterized by N₂ adsorption at 77 K using a
136 surface area analyzer (Micromeritics, ASAP-2020, USA), and the surface areas (S_{BET}) of
137 CACs were calculated from the isotherms using the Brunauer-Emmett-Teller (BET)
138 equation. The total pore volume (V_t) was calculated by converting the adsorption amount at
139 P/P₀ = 0.95 to a volume of liquid adsorbate. The external area (A_a), micropore area (A_m)
140 and volume (V_m) were obtained using the t-plot method.

141 Different CACs samples were also analyzed with Fourier transform infrared
142 spectrometer (Magna-IR 750), the samples were mixed with KBr powder and the mixtures
143 were press into pellet. The spectra were recorded from 4000 to 400 cm⁻¹. The spectra were
144 obtained with a resolution of 1 cm⁻¹, 10 scans per spectrum are used in FTIR
145 measurements.

146 The pH_{pzc} of CACs was determined by a mass titration method proposed by Noh and
147 Schwarz [18], which is defined as the pH of the mixtures at which surface charge density
148 on the adsorbent is zero. CAC (0.1 g) was added to 50 mL of 0.01 mol/L NaCl solutions,
149 then, the pH had been adjusted to a set value between 2 and 12 with NaOH or HCl. The
150 flasks were sealed and placed on a shaker for 48 h. The pH_{pzc} is the point where
151 pH_{final}-pH_{inital} = 0.

152 The study of the surface functional groups was based on the Boehm titration method [19].
153 The basic groups were neutralized with HCl solution (0.05 mol L⁻¹). The various acidic
154 groups were determined under two assumptions, as follow: NaHCO₃ neutralized carboxyl

155 groups, NaOH neutralized carboxyl, lactone and phenolic groups and Na₂CO₃ neutralized
156 carboxyl and lactone groups. An amount of 1.0 g of CAC was added to the 25.00 mL
157 solution of one of the three 0.05 M reaction bases (NaHCO₃, Na₂CO₃ and NaOH). The
158 solutions were then sealed and placed in a shaker for 48 h at 30 °C.

159 **2.4. Adsorption studies**

160 **2.4.1. Adsorption performance analysis**

161 Given the low solubility of PAHs in water, the use of ethanol as co-solvent was efficient
162 for the solubilization of the naphthalene in the aqueous medium. Naphthalene was initially
163 solved into ethanol aqueous solution (30 vol%) to prepare the stock solutions. The
164 concentrations of adsorbate solutions were measured by a UV-75N spectrophotometer at
165 $\lambda_{\max} = 218$ nm.

166 For the adsorption experiment, 100 mL of the 30 mg L⁻¹ naphthalene solution was placed
167 in a 250 mL conical flask. 15 mg of CAC prepared was added into the solution. The
168 solution was then shaken for 60 min at 20 °C. The amount of the adsorbate (Q_e) was
169 calculated as follow:

$$170 \quad Q_e = \frac{(C_0 - C_e)V}{m} \quad (1)$$

171 where C_0 (mg L⁻¹) and C_e (mg L⁻¹) are liquid-phase concentrations of naphthalene at initial
172 and equilibrium, respectively. V (mL) represents the volume of the solution and m (g)
173 stands for the mass of CAC used.

174 **2.4.2. Adsorption kinetics**

175 In the adsorption kinetic experiments, 100 mL of the 30 mg L⁻¹ naphthalene solution
176 containing 15 mg of the CAC was placed in 250 mL conical flask. The solution was then

177 shaken for various times at 20 °C.

178 The pseudo-first-order, pseudo-second-order and intraparticle diffusion models were
179 applied for analyzing the experimental data.

180 The pseudo-first-order kinetic rate equation is expressed as [20]:

$$181 \quad \frac{1}{Q_t} = \frac{1}{Q_e} + \frac{k_1}{Q_e t} \quad (2)$$

182 where k_1 is the rate constant of pseudo-first-order sorption (min), which can be determined
183 from the slope of the linearized pseudo-first-order rate equation, Q_e and Q_t (mg g^{-1}) are the
184 adsorption capacities at equilibrium and time t , respectively.

185 The pseudo-second-order kinetic rate equation is expressed as [20]:

$$186 \quad \frac{t}{Q_t} = \frac{1}{k_2 Q_e^2} + \frac{t}{Q_e} \quad (3)$$

187 where k_2 is the second-order rate constant ($\text{g mg}^{-1} \text{min}^{-1}$) can be determined from the
188 intercept of the linearized pseudo-second-order rate equation.

189 In the intraparticle diffusion model, the relationship between the adsorption capacity at time
190 t , Q_t and $t^{1/2}$ could be written as [20]:

$$191 \quad Q_t = K_p t^{1/2} + C \quad (4)$$

192 where K_p is the intraparticle diffusion constant ($\text{mg g}^{-1} \text{min}^{-1/2}$) and C is the intercept of the
193 line, which is proportional to the boundary layer thickness.

194 **2.4.3. Adsorption isotherm**

195 For the adsorption isotherms experiments, 15 mg CAC and 100 mL various initial
196 concentration of naphthalene solution ($20\text{-}70 \text{ mg L}^{-1}$) were placed in a set of 250 mL
197 conical flasks. Then the solution was shaken for 60 min at 20 °C.

198 The Langmuir adsorption Eq. (5), predicts the existence of monolayer coverage of the
199 adsorbate at the outer surface of the adsorbent [11].

$$200 \quad \frac{C_e}{Q_e} = \frac{1}{q_m K_L} + \frac{C_e}{q_m} \quad (5)$$

201 where C_e and Q_e are as defined in Eq. (1), q_m is adsorption maximum (mg g^{-1}); K_L is
202 sorption equilibrium constant (L mg^{-1}).

203 The Freundlich isotherm [11] is an empirical equation employed to describe
204 heterogeneous systems, and is expressed by the following Eq. (6):

$$205 \quad \log Q_e = \frac{1}{n} \log C_e + \log K_F \quad (6)$$

206 where K_F is a constant which represents a measure of the adsorption capacity of the
207 adsorbent for specific solute, and n is a measure of intensity of adsorption.

208 The Temkin model considers the effects of some indirect adsorbent-adsorbate
209 interactions on an adsorption isotherm, because of these interactions, the heats in adsorption
210 would more often decrease than increase with increasing coverage [21]. This equation has
211 the form:

$$212 \quad Q_e = B \ln C_e + B \ln a \quad (7)$$

213 where the term B corresponds to RT/b , T is absolute temperature (T), R is the gas constant
214 (L g^{-1}), b is the Temkin constant related to the heat of sorption (kJ mol^{-1}), and C_e is the
215 equilibrium concentration (mg L^{-1}).

216 **3. Results and discussion**

217 **3.1. Effect of microwave power on naphthalene adsorption on CACs**

218 The CACs were prepared with a coal alkali ratio of 1:2 at a radiation time of 10 min.

219 When the microwave power was at 300 W, the pore structures had not adequately
220 developed, and the adsorption amount was small, however, the adsorption capacity showed
221 a drastic increase with the increase of microwave power (Fig. 1); such a phenomenon could
222 be ascribed to the combined effect of internal and volumetric heating, which expanded the
223 carbon structure [22]. However, if microwave power is higher than 700 W, over-gasification
224 might cause the destruction of pore structures, thereby progressively decreasing adsorption
225 capability. Moreover, exorbitant temperatures might produce local hotspots, leading to
226 external ablation, shrinkage and collapse of the carbon framework, and consequently
227 reducing the accessibility of active sites. Therefore, the microwave power levels proposed
228 were at 500 and 700 W for the effective activation of the ACAC (LCAC) and BCAC,
229 respectively. Porosity development may depend on ash. Indeed, mineral matter is known to
230 act as a catalyst to accelerate gasification reactions during activation processes [23].
231 Furthermore, the release of volatile matter favors porosity development. The adsorption
232 amounts of naphthalene on the CACs prepared under the optimum power level followed the
233 order: ACAC > BCAC > LCAC. This result may be due to the fact that A-coal has lower
234 contents of volatile matter and ash than B-coal and L-coal [24]. Thus, A-coal is a more
235 suitable raw material for CACs production than B-coal and L-coal.

236 **Fig. 1 should be positioned here.**

237 **3.2. Characterization of CACs**

238 3.2.1. Element contents analysis

239 According to the results, the three CACs had similar elemental compositions (Table 1).

240 The carbon content of the CACs pronouncedly increased after activation. On the contrary,

241 the oxygen content was decreased in CACs. Meanwhile, the C/O ratios increased from 2.81,
242 2.49, 2.39 for the A-coal, B-coal and L-coal to 4.58, 4.42 and 4.26 for the ACAC, BCAC,
243 LCAC, respectively, this could be due to some oxygen-containing groups were eliminated
244 from the carbon surface. Meanwhile, the content of nitrogen and sulfur also had a certain
245 decrease.

246 3.2.2. XPS analysis

247 The survey spectra of the CACs contained distinct peaks for carbon and oxygen and
248 weak peaks for nitrogen (Fig. 2). It can be seen that the C content increased while the
249 contents of O decreased after microwave treatment, implying the elimination of the oxygen
250 groups of CACs during the activation process.

251 **Fig. 2 should be positioned here.**

252 3.2.3. Surface morphology

253 SEM images of the coals and CACs are shown in Fig. 3. It showed that the surfaces
254 of the coals are fairly smooth without any pores. After activation, the external surfaces of
255 the three CACs exhibited a highly pronounced and almost irregular pore structure. Reaction
256 (1) to result in the widening the existing pores by the internal structure of carbon matrix and
257 to create new porosities [25], as follows:



259 **Fig. 3 should be positioned here.**

260 3.2.4. Textural structure

261 The isotherms demonstrated a sharp rise at the low P/P_0 range, and a gradual increase at
262 the relatively high P/P_0 range (Fig. 4). According to the IUPAC classification system, all

263 the adsorption isotherms belonged to type I, thereby indicating that all the CACs were
264 mainly micropores. The desorption branch presents a small hysteresis loop at high relative
265 pressures, thereby indicating the presence of mesoporosity. This adsorption behavior
266 suggests a combination of microporous-mesoporous structure. Among the samples, the
267 ACAC showed the best developed porosity. Such porous features may be ideally adapted for
268 the removal of aromatics from an aqueous phase. The BET surface area and pore volume of
269 the ACAC were evaluated as $1450.28 \text{ m}^2 \text{ g}^{-1}$ and $0.66 \text{ cm}^3 \text{ g}^{-1}$, respectively (Table 2),
270 which are both larger than those of BCAC and LCAC. This finding may be due to the high
271 ash levels of B-coal and L-coal (Table 1), given that ashes do not contribute to porosity,
272 high ash levels in the precursor naturally lead to reduced pore volumes [24]. In addition,
273 when a small amount of volatile overflows, the left pore channels play an important role in
274 the activation process, which obviously promotes pore development of CACs,
275 however, highly volatile coal will lead to agglomeration during carbonization, and a large
276 amount of volatile gas discharge increases the processing load, generally, less than 10% of
277 the volatile matter is beneficial [26]. And these are directly related to its adsorptive capacity,
278 which is corresponding with the previous adsorption results.

279 **Fig. 4 should be positioned here.**

280 **Table 2 should be positioned here.**

281 3.2.5. Surface chemistry features of CACs

282 ACAC has a higher pH_{PZC} value and more basic groups than BCAC and LCAC (Table
283 3). Moreover, ACAC has less number of acidic functional groups than BACA and LCAC.
284 These results could be due to the different physical properties of the raw coals. Furthermore,
285 ACAC achieved the largest naphthalene adsorption amount among the CACs. It could be

286 concluded the decrease of acid oxygen-containing functional groups and the increase of
287 basic groups in the ACAC could enhance the adsorption amount of naphthalene.

288 **Table 3 should be positioned here.**

289 3.2.6. FTIR spectra of CACs

290 The three CACs showed similar FTIR spectra (Supporting information Fig. S1),
291 indicating that they have identical species of functional groups on the surface. The broad
292 band at approximately 3450 cm^{-1} is assigned to the O-H stretching vibration of the
293 hydroxyl functional groups, including hydrogen bonding [27]. The peak is less pronounced
294 in the ACAC sample than in the other samples, implying the presence of a lower number of
295 -OH groups in the carboxylic groups of ACAC than in those of BCAC and LCAC. As
296 observed among the samples, ACAC had the lowest number of acid oxygen-containing
297 functional groups. The minimal acidic oxygen functional groups such as phenols and
298 carboxyls of the CACs may enhance the adsorption capacity of naphthalene from the
299 aqueous solution, as shown in the results of the acid-base titration.

300 **3.3. Adsorption kinetics of naphthalene on CACs**

301 The adsorption kinetics of naphthalene is shown in Fig. 5. The kinetic models of
302 pseudo-first-order, pseudo-second-order, and intraparticle diffusion were tested to correlate
303 the experimental kinetic data of naphthalene on the three CACs (Table 4). The three CACs
304 appeared to have similar behaviors in terms of kinetics. The adsorption process has two
305 stages: at the first stage, naphthalene is rapidly adsorbed onto the easily accessible
306 hydrophobic sites within the first 20- min period. At the second stage, the uptake is
307 probably limited by the slower migration of naphthalene to less accessible sites associated
308 with mesopores, thus taking a longer adsorption time. Yuan et al. [14] reported similarly

309 that the adsorption process of PAHs onto petroleum coke-derived porous carbon also was
310 the two-stage. In addition, the adsorption rate constants of ACAC determined are higher
311 than that of BCAC and LCAC. This is due to that ACAC has higher surface area, more
312 abundant sorption sites and superior distribution of pore sizes than BCAC and LCAC
313 (Table 2 and Fig. 4). An ideal percentage of pores of ACAC in the mesopore and macropore
314 (20–500 Å) size ranges could be minimized the kinetic diffusion resistance during the
315 adsorption process [28].

316 The pseudo-second-order model had higher R^2 and Q_{exp} values that were closer to the
317 experimental values than the pseudo-first-order and intraparticle diffusion models. The
318 pseudo-second-order model demonstrated better fitting for all three CACs than the others.
319 Cabal et al. [7] also found the experimental data of adsorption kinetics of aqueous
320 naphthalene on the AC from bean pods were fitted to the pseudo-second kinetic model well.
321 The adsorption mechanism and the potential rate-determining steps of naphthalene on
322 CACs could be involved in mass transport and chemical reaction processes [21]. In addition,
323 ACAC has higher mesopore volume, which is supported that intraparticle diffusion could
324 be involved in the sorption process of naphthalene on CACs. However, it was not the only
325 rate-determining step.

326 **Fig. 5 should be positioned here.**

327 **Table 4 should be positioned here.**

328 **3.4. Adsorption isotherm of CACs**

329 The adsorption isotherms of naphthalene from the solution on CACs are depicted in Fig.
330 S2 (Supporting information). Table 5 lists the parameters of the Langmuir, Freundlich and
331 Temkin adsorption isotherm models of naphthalene on three CACs at 20 °C, along with

332 their regression coefficients (R^2). Compared with Langmuir and Temkin, the equilibrium
333 data was well represented by the Freundlich equation. Similarly, Yuan et al. [14] reported
334 that the equilibrium adsorption isotherms of naphthalene from water on petroleum
335 coke-derived porous carbon was fitted the Freundlich equation well. This indicates that the
336 adsorption of naphthalene onto CACs is heterogeneous and may not be confined to a
337 monolayer adsorption. As shown in Table 5, “ $1/n$ ” values are between 0.1 and 1, thereby
338 indicating a favorable adsorption [21]. Since naphthalene is nonpolar compounds, this
339 observation indicates a strong hydrophobic interaction between the CAC and naphthalene
340 with a favorable adsorption [16].

341 **Table 5 should be positioned here.**

342 **3.5. Effect of CACs’ surface characteristics on naphthalene adsorption**

343 The adsorption amount of the adsorbate on CACs is generally related to the CACs’
344 surface characteristics, texture and surface physicochemical properties. Results (Fig. S3
345 Supporting information) showed that obtaining a well-developed total pore volume, high
346 surface area, low oxygen content, and a high basic functional group is necessary to improve
347 the adsorption capacity towards naphthalene on CACs.

348 **4. Conclusions**

349 Three kinds of ACs were prepared from typical coals in Xinjiang using microwave
350 radiation. Our results indicate that microwave heating is an effective method for the
351 processes involved. The BET surface area and pore volume of ACAC (obtained at 700 W)
352 were higher than those of BCAC and LCAC. For CACs, the presence of microporous-
353 mesoporous structures enhanced the specific naphthalene adsorption. The FTIR spectra
354 suggested that the CACs had similar functional groups on the surface, and that of ACAC

355 contained higher number of basic functional groups and higher pH_{PZC} than the other
356 samples. The ACAC had a lower number of acid oxygen-containing groups. The results
357 agreed with those obtained from acid-base titration. In addition, raw coal with a low content
358 of ash and volatile matter was suitable for the preparation of ACs. For the three CACs, the
359 Freundlich isotherm model described the equilibrium data well. The optimum adsorption
360 capacity towards naphthalene on the ACAC was 167.01 mg g^{-1} . Moreover, the adsorption
361 kinetics fits very well to the pseudo-second-order model. Among the three coals, anthracite
362 coal is the best material for the preparation of CACs for naphthalene adsorption.

363 **Acknowledgements**

364 This work was supported financially by funding from the National Natural Science
365 Foundation of China (51262025) and International scientific and technological cooperation
366 project of Xinjiang Bingtuan (2013BC002).

367

368

369

370

371

372

373

374

375

376

377 **References**

- 378 [1] Wang TH, Tan SX, Liang CH. Preparation and characterization of activated carbon
379 from wood via microwave-induced $ZnCl_2$ activation. *Carbon* 2009; 47:1867-5.
- 380 [2] Foo KY and Hameed BH. Utilization of rice husks as a feedstock for preparation of
381 activated carbon by microwave induced KOH and K_2CO_3 activation. *Bioresour*
382 *Technol* 2011; 102:9814-7.
- 383 [3] Duan XH, Srinivasakannan C, Peng J H, Zhang L B, Zhang ZY. Preparation of
384 activated carbon from *Jatropha* hull with microwave heating: Optimization using
385 response surface methodology. *Fuel Process Technol* 2011; 92:394-0.
- 386 [4] Foo KY and Hameed BH. Preparation and characterization of activated carbon from
387 pistachio nut shells via microwave-induced chemical activation. *Biomass Bioenerg*
388 2011^a; 35:3257-1.
- 389 [5] Sudaryanto Y, Hartono SB, Irawaty W, Hindarso H, Ismadji S. High surface area
390 activated carbon prepared from cassava peel by chemical activation. *Bioresour Technol*
391 2006; 97:734-9.
- 392 [6] Liu QS, Zheng T, Wang P, Guo Liang. Preparation and characterization of activated
393 carbon from bamboo by microwave-induced phosphoric acid activation. *Ind Crop Prod*
394 2010; 31:233-8.
- 395 [7] Cabal B, Budinova T, Ania CO, Tsyntsarski B, Parra JB, Petrova B. Adsorption of
396 naphthalene from aqueous solution on activated carbons obtained from bean pods. *J*
397 *Hazard Mater* 2009; 161:1150-6.
- 398 [8] Duan XX, Srinivasakannan C, Qu WW, Wang X, Peng JH, Zhang LB. Regeneration of

- 399 microwave assisted spent activated carbon: Process optimization. adsorption isotherms
400 and kinetics, Chem Eng Process 2012; 53:53-2.
- 401 [9] Ji YB, Li TH, Zhu L, Wang XX, Lin QL. Preparation of activated carbons by
402 microwave heating KOH activation. Appl Surf Sci 2007; 254:506-2.
- 403 [10] Huang LH, Sun YY, Wang WL, Yue QY, Yang T. Comparative study on
404 characterization of activated carbons prepared by microwave and conventional heating
405 methods and application in removal of oxytetracycline (OTC). Chem Eng J 2011;
406 171:1446-3.
- 407 [11] Wassenberg DM and Di Giulio RT. Synergistic embryotoxicity of polycyclic aromatic
408 hydrocarbon aryl hydrocarbon receptor agonists with cytochrome P4501A inhibitors in
409 *Fundulus heteroclitus*. Environ Health Persp 2004; 112:1658-4.
- 410 [12] Xia XH, Yu H, Yang ZF, Huang GH. Biodegradation of polycyclic aromatic
411 hydrocarbons in the natural waters of the Yellow River: Effects of high sediment
412 content on biodegradation. Chemosphere 2006; 65:457-6.
- 413 [13] Liu JJ, Wang XC, Fan B. Characteristics of PAH adsorption on inorganic particles and
414 activated sludge I domestic wastewater treatment. Bioresour Technol 2011;
415 102:5305-1.
- 416 [14] Yuan MJ, Tong ST, Zhao SQ, Jia CQ. Adsorption of polycyclic aromatic
417 hydrocarbons from water using petroleum coke-derived porous carbon. J Hazard Mater
418 2010; 181:1115-0.
- 419 [15] Iovino P, Canzano S, Capasso S, Di Natale M, Erto A, Lama A, Musmarra D. Single
420 and competitive adsorption of toluene and naphthalene onto activated carbon. Chem
421 Eng Transactions. 2013; 32,67-72.
- 422 [16] Ge XY, Tian F, Wu ZL, Yan YJ, Cravotto G, Wu ZS. Adsorption of naphthalene from

423 aqueous solution on coal-based activated carbon modified by microwave induction:
424 Microwave power effects. Chem Eng Process 2015; 91:67-7.

425 [17] Xiao XM, Tian F, Yan YJ, Wu ZS. Adsorption behavior of pyrene onto coal-based
426 activated carbon prepared by microwave activation. Journal of Shihezi University
427 (Natural science) 2014; 32:486-0.

428 [18] Noh JS and Schwarz JA. Estimation of the point of zero charge of simple oxides by
429 mass titration. J Colloid Interface Sci 1989; 130:157-164.

430 [19] Boehm HP. some aspects of the surface chemistry of carbon blacks and other carbons,
431 Carbon 1994; 32:759-9.

432 [20] Atul V, Maldhure Ekhe JD. Preparation and characterizations of microwave assisted
433 activated carbons from industrial waste lignin for Cu (II) sorption. Chem Eng J 2011;
434 168:1103-1.

435 [21] Vidal CB, Barros AL, Moura CP, de Lima AC, Dias FS, Vasconcellos LC, Fechine PB,
436 Nascimento RF. Adsorption of polycyclic aromatic hydrocarbons from aqueous
437 solutions by modified periodic mesoporous organosilica. J Colloid Interface Sci 2011;
438 357:466-3.

439 [22] Emamia Z and Azizianb S. Preparation of activated carbon from date sphate using
440 microwave irradiation and investigation of its capability for removal of dye pollutant
441 from aqueous media. J Anal Appl Pyrol 2014; 108:176-4.

442 [23] Tellez-Juárez MC, Fierro V, Zhao W, Fernández-Huerta N, Izquierdo MT, Reguera E,
443 Celzard A. Hydrogen storage in activated carbons produced from coals of different
444 ranks: Effect of oxygen content. Int J Hydrogen Energ 2014; 39:4996-2.

445 [24] Cui H, Cao Yan, Pan WP. Preparation of activated carbon for mercury capture from
446 chicken waste and coal. *J Anal Appl Pyrolysis* 2007; 80:319-4.

447 [25] Ahmed MJ and Theydan SK. Optimization of microwave preparation conditions for
448 activated carbon from Albizia lebbeck seed pods for methylene blue dye adsorption. *J*
449 *Anal Appl Pyrol* 2014; 105:199-8.

450 [26] Xing BL, Huang GX, Chen LJ, Zhang CX, Wang L. Preparation and characterization
451 of high quality low-rank coal based activated carbon. *Journal of China Coal Society*
452 2013; 38:218-2.

453 [27] Liu QS, Zheng T, Wang P, Guo L. Preparation and characterization of activated
454 carbon from bamboo by microwave-induced phosphoric acid activation. *Ind Crop Prod*
455 2010; 31:233-8.

456 [28] Bu J, Loh G, Gwie CG, Dewiyanti S, Tasrif M, Borgna A. Desulfurization of diesel
457 fuels by selective adsorption on activated carbons: Competitive adsorption of
458 polycyclic aromatic sulfur heterocycles and polycyclic aromatic hydrocarbons. *Chem*
459 *Eng J* 2011; 66:207-7.

460

461

462

463

464

465

466

467

468

469

470

471

472

473 **Figure captions:**

474 Fig. 1 Adsorption amount of naphthalene on the ACAC, BCAC and LCAC prepared using
475 various microwave power levels ($C_0= 30 \text{ mg g}^{-1}$).

476 Fig. 2 XPS survey spectra of raw coals and CACs.

477 Fig. 3 SEM micrographs of the raw coals and CACs at 5000 \times magnification.

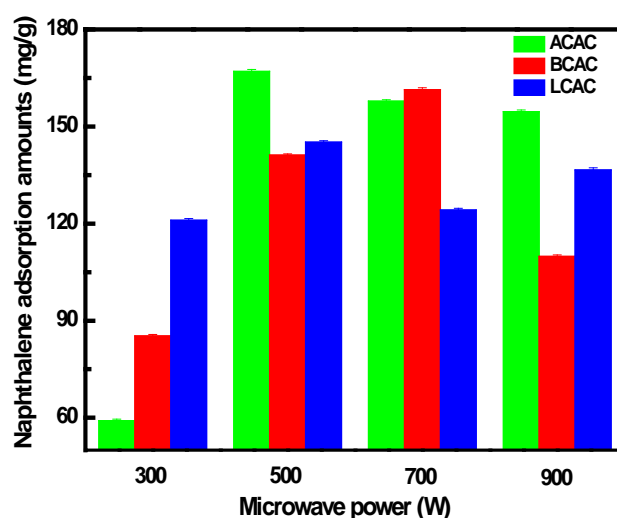
478 Fig. 4 N_2 adsorption/desorption isotherms at 77 K (a) and pore size distribution (b).

479 (ACAC and LCAC under microwave power of 500 W and BCAC under 700 W).

480 Fig.5 Adsorption kinetics of naphthalene on CACs ($C_0= 30 \text{ mg L}^{-1}$, 20 $^\circ\text{C}$).

481

482



483

484 Fig.1. Adsorption amount of naphthalene on the ACAC, BCAC and LCAC prepared
485 using various microwave power levels ($C_0= 30 \text{ mg g}^{-1}$).

486

487

488

489

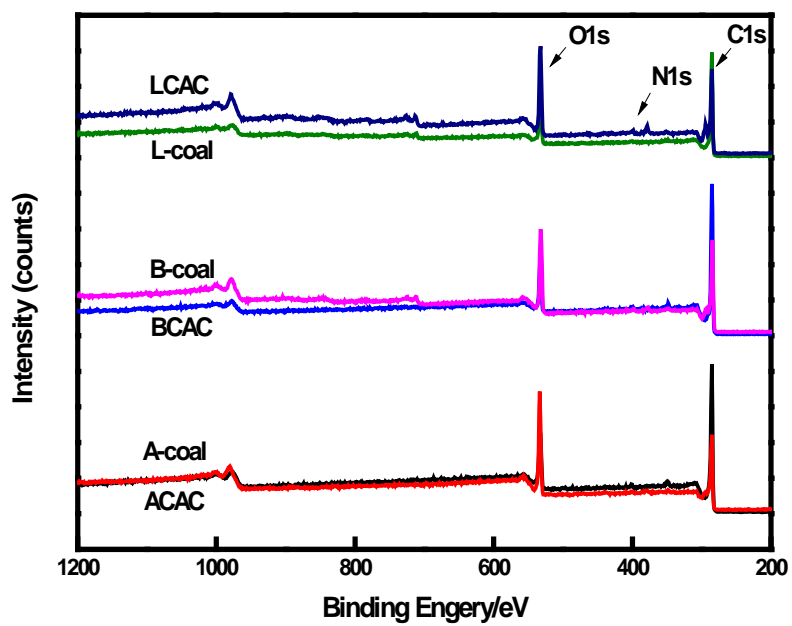
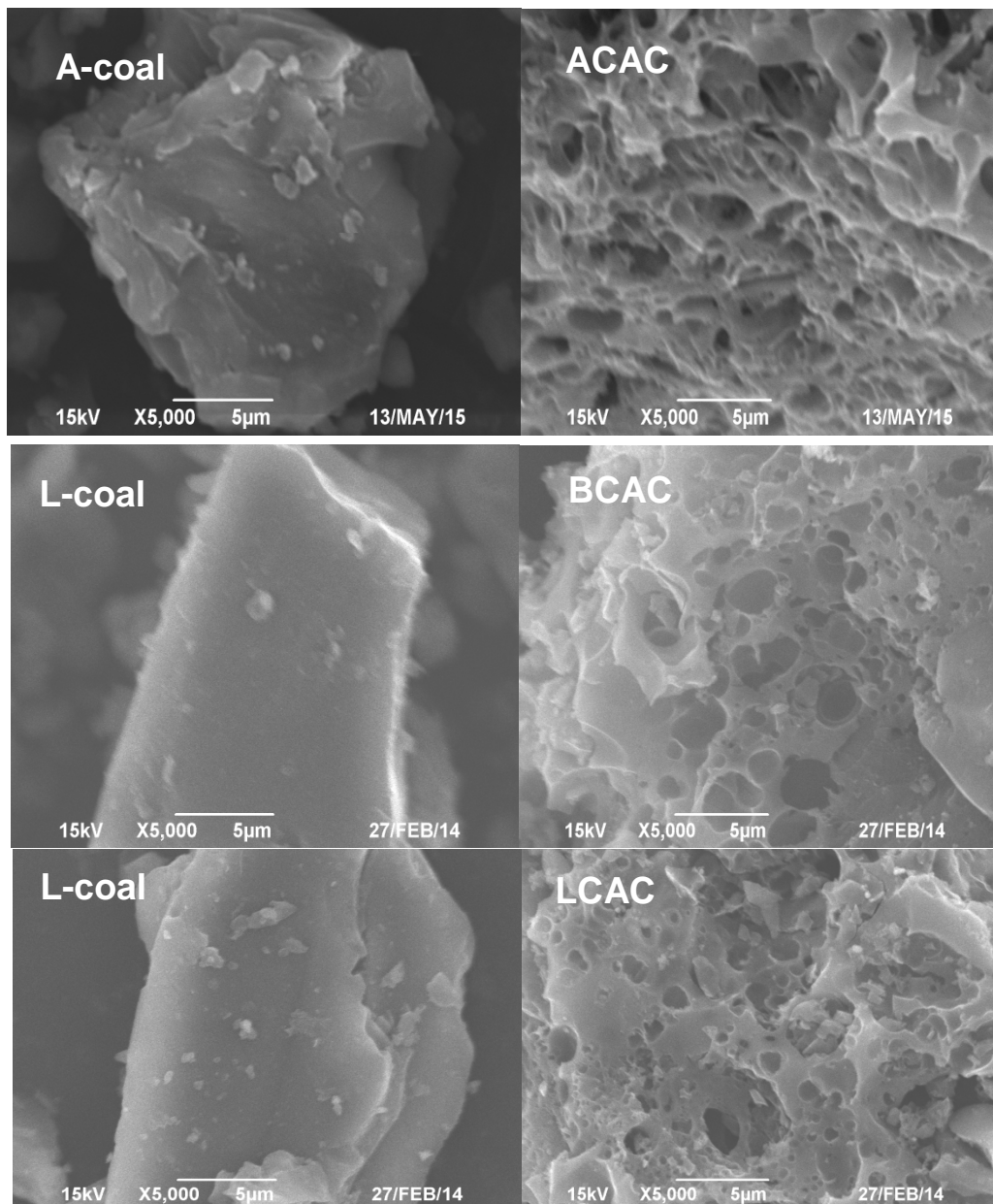


Fig. 2. XPS survey spectra of raw coals and CACs.

490
491
492
493
494
495
496
497
498
499
500
501
502
503
504
505
506
507



508

509

510

511

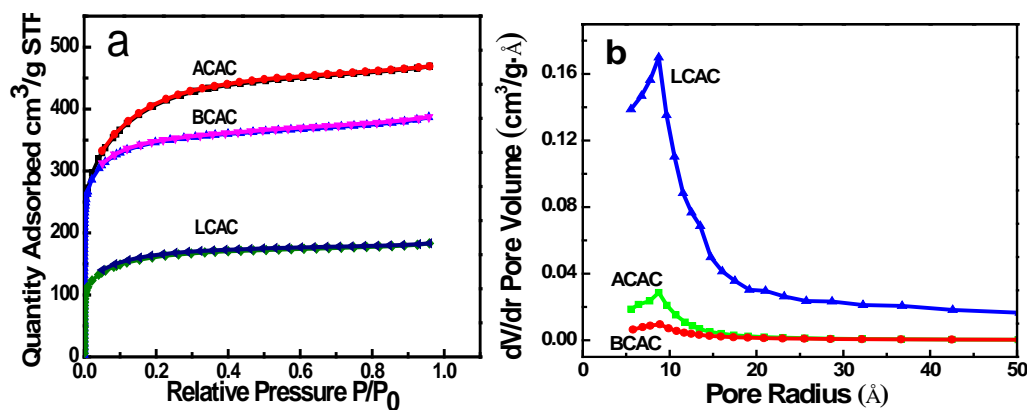
512

513

514

515

Fig. 3. SEM micrographs of the raw coals and CACs at 5000× magnification.



516

517

Fig.4. N₂ adsorption/desorption isotherms at 77 K (a) and pore size distribution (b).

518

(ACAC and LCAC by microwave power of 500 W and BCAC by 700 W)

519

520

521

522

523

524

525

526

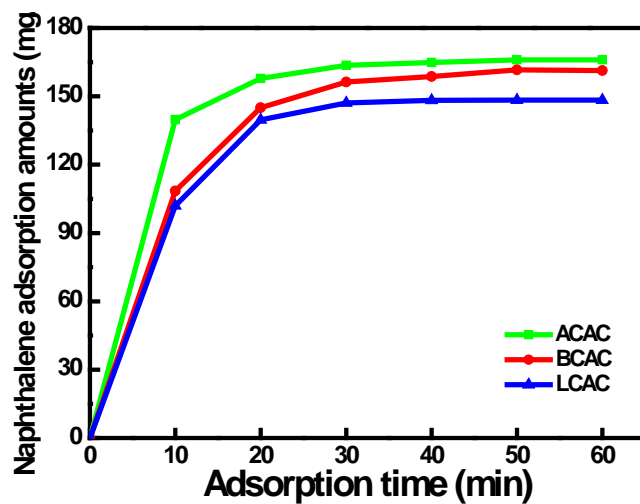
527

528

529

530

531



532

533

Fig. 5. Adsorption kinetics of naphthalene on CACs ($C_0= 30 \text{ mg L}^{-1}$, $20 \text{ }^\circ\text{C}$).

534

535

536

537

538

539

540

541

542

543

544

545

546

547

548

549 Table 1 Characteristics of coals selected and atomic content of the coals and CACs.

Samples	Moisture %	Ash %	Volatile %	Fixed carbon %	Atom content %					
					C	H	N	S	O _{diff}	C/O
A-coal	9.00	4.21	24.98	61.81	70.75	3.18	0.68	0.25	25.14	2.81
B-coal	9.10	6.01	31.60	53.29	67.58	4.30	1.00	0.05	27.07	2.49
L-coal	2.10	6.10	38.8	53.0	66.12	5.01	1.22	0.06	27.59	2.39
ACAC	-	5.20	-	-	80.25	1.14	0.95	0.13	17.53	4.58
BCAC	-	8.01	-	-	78.68	2.23	1.21	0.08	17.80	4.42
LCAC	-	8.12	-	-	77.35	2.90	1.45	0.15	18.15	4.26

550

551

552

553

554

555

556

557

558

559

560

561 Table 2 Surface characteristics of the prepared CACs.

Samples	Microwave power W	S _{BET} (m ² g ⁻¹)	A _m (m ² g ⁻¹)	A _e (m ² g ⁻¹)	V _{mic} (cm ³ g ⁻¹)	V _{mes} (cm ³ g ⁻¹)	V _t (cm ³ g ⁻¹)	V _{mic} /V _{mes} (%)	Average pore radius
									(Å)
ACAC	500	1450.28	614.36	835.92	0.26	0.40	0.66	26/40	13.72
BCAC	700	1209.99	869.35	340.64	0.38	0.17	0.55	38/17	18.08
LCAC	500	570.52	337.57	232.95	0.15	0.11	0.26	15/11	15.54

562 S_{BET}: specific surface area obtained by BET equation, A_m, A_e: micropore area, external surface area, V_{mic}, V_{mes}, V_t:

563 micropore volume, mesoporous volume, total pore volume.

564

565

566

567

568

569

570

571

572 Table 3 Surface chemistry of the CACs

Samples	Lactone (mmol g ⁻¹)	Phenolic (mmol g ⁻¹)	Carboxyl (mmol g ⁻¹)	Total acidic (mmol g ⁻¹)	Basic (mmol g ⁻¹)	pH _{PZC}
ACAC	0.4006	0.0013	0.0047	0.4066	5.1250	7.35
BCAC	0.3924	0.0307	0.0120	0.4351	4.7900	7.21
LCAC	0.3815	0.0633	0.0233	0.4681	3.9250	7.15

573
574
575
576
577
578
579
580
581
582
583
584
585
586
587
588
589
590
591
592
593
594
595
596

597 Table 4 kinetic model parameters for the adsorption of naphthalene on the CACs.

Samples	Q_{exp} (mg g ⁻¹)	Pseudo-first-order kinetic model			Pseudo-second-order kinetic model			Intraparticle diffusion model	
		k_1 (min ⁻¹)	Q_e (mg g ⁻¹)	R^2	k_2 (g mg ⁻¹ min ⁻¹)	Q_e (mg g ⁻¹)	R^2	k_p (mg g ⁻¹ min ^{1/2})	R^2
ACAC	167.01	2.3333	165.67	0.980	0.0033	166.71	0.999	8.9770	0.830
BCAC	161.36	2.2568	161.21	0.968	0.0014	161.37	0.997	4.0300	0.860
LCAC	145.15	2.0594	147.10	0.929	0.0019	144.68	0.996	8.9400	0.679

598
599
600

601 Table 5 Isotherm constants for the adsorption of naphthalene in aqueous solution onto the
 602 CACs at 20 °C.

Samples	Langmuir			Freundlich			Temkin		
	$K_L(\text{L mg}^{-1})$	$q_m(\text{mg g}^{-1})$	R^2	$K_F(\text{L g}^{-1})$	$1/n$	R^2	B	K_t	R^2
ACAC	0.32	166.67	0.982	69.48	0.44	0.992	29.29	1.16	0.973
BCAC	0.13	156.28	0.980	32.39	0.58	0.995	26.52	0.41	0.988
LCAC	0.06	150.00	0.998	12.58	0.76	0.999	26.66	0.21	0.992

603

604